RSC Advances

PAPER

View Article Online
View Journal | View Issue

Cite this: *RSC Adv.*, 2023, **13**, 2090

Silica supported lanthanum trifluoroacetate and trichloroacetate as an efficient and reusable water compatible Lewis acid catalyst for synthesis of 2,4,5-triarylimidazoles *via* a solvent-free green approach†

Dnyaneshwar Purushottam Gholap, Ramdas Huse, Sudarshan Dipake and Machhindra K. Lande *

Received 5th November 2022
Accepted 10th December 2022

DOI: 10.1039/d2ra07021a

rsc.li/rsc-advances

In the present research article, we have developed solid heterogenous silica supported lanthanum trifluoroacetate and trichloroacetate as green Lewis acid catalysts. These catalysts were synthesized by a novel, simple, cheap, clean, and environment friendly method. The physicochemical properties of the prepared catalysts were well studied and characterized by sophisticated spectroscopic techniques such as FTIR, TGA, XRD, EDX, SEM, TEM and BET analysis. The catalyst was utilized in the synthesis of arylimidazole derivatives *via* green protocols under solvent-free conditions at 70 °C with a higher yield, mild reaction conditions and a short reaction time. The catalyst works superiorly in water as well as in various organic solvents as a reusable and easily recoverable catalyst.

1. Introduction

Heterogeneous catalysts are considered as a building block, rapidly growing and emerging area in the field of catalysis to promote diverse reactions.[1] The development and design of novel heterogeneous catalysts are in high demand due to their wide range of applications in organic transformations in various fields of green chemistry.[2–4] The heterogenous catalysts show several advantages such as reusability and recyclability with easy processability compared to homogenous catalysts.[5] The Lewis acid catalysts having chemical stability, thermal stability and inherent Lewis acidity are well known for promoting numerous reactions including biomass conversion, biodiesel production and synthesis of both natural and synthetic organic molecules.[6] Lewis acid catalysed reactions have a great scope due to their distinctive reactivity, selectivity and mild reaction conditions.[7,8]

In 1991, the first ever water compatible Lewis acid lanthanide triflate was revealed by Kobayashi.[9] lanthanide triflates have been literature known compound at that time however their role and use in organic transformations have been restrained. Prior to it, lanthanide triflate was used as homogeneous catalysts for the synthesis of amidine in anhydrous organic solvent.[10] Until this synthesis, it was widely assumed that Lewis acid catalysis required to be carried out in a completely anhydrous state. The major distinguishing characteristics of lanthanide triflates are that they are stable and operate as Lewis acids in water. Following this first report, not only homogeneous lanthanide triflates but also rare earth metal triflates that are water-compatible Lewis acids were reported.[11] In recent times, silica supported lanthanide triflates, rare earth metal triflates and silica supported trifluoroacetic acid or trichloroacetic acid heterogenous Lewis acid catalysts were developed and utilized in many organic transformations.[12,13] These heterogeneous Lewis acid catalysts carry out a variety of useful reactions and have a number of notable advantages, making them environmentally friendly green Lewis acid catalysts.[14] This unique properties of green Lewis acid catalysts have also made them ideal alternatives to the conventional Lewis acid catalysts, since they are needed in a stoichiometric amount, stable and function as Lewis acid in both water and organic solvents, found to be water-competent, easily retrieved and reused after a reaction without losing their catalytic activity.[15] Moreover, these green Lewis acids are highly efficient chemoselective, regioselective and stereoselective catalysts for different series of organic transformations.[16]

However, both homogeneous and heterogeneous lanthanide triflates and rare earth metal triflates catalyst have several limitations and restrictions, mainly they are highly sensitive to moisture and hygroscopic in nature, require strict storage under anhydrous, moisture-free, and dry conditions. They are also expensive catalysts in terms of price, and their synthesis required specific inert reaction condition. To overcome these

Department of Chemistry, Dr Babasaheb Ambedkar Marathwada University, Aurangabad, Maharashtra, India. E-mail: mkl_chem@yahoo.com

† Electronic supplementary information (ESI) available. See DOI: https://doi.org/10.1039/d2ra07021a

problems, we have developed silica supported lanthanum trifluoroacetate and trichloroacetate Lewis acid catalysts as a competent alternative for the lanthanide triflates and rare earth metal triflates catalysts. The presently synthesized silica supported catalysts are nonhygroscopic, moisture insensitive and less expensive as they are prepared by commercially available starting materials at normal reaction conditions. Further, they are required in a stoichiometric amount, stable, and function as Lewis acid in both water and organic solvents, and found to be water competent. They can also be easily recovered and reused after a reaction without losing their catalytic activity.

In recent years, imidazole-containing heterocycles have very high demands as they are present in a wide spectrum of bioactive compounds with a variety of medicinal and biological applications. The imidazole nucleus has been found in a variety of pharmacologically active compounds, including histamine and histidine hormone.[17] Notably, imidazole nuclei can be found in a variety of pharmacologically active molecules, such as eprosartan,[18] losartan,[19] and clotrimazole,[20] alpidem,[21] flumazenil.[21] However, a variety of heterocyclic frameworks containing imidazole cores have piqued our interest due to their biological actions and importance in therapeutics and medicine.[22,23] In this context, the synthesis of a five-membered nitrogen-containing ring structure is still a hot topic. A literature survey of several methods for the synthesis of highly functionalized tetra- and trisubstituted imidazole scaffolds reveals that[24–29] some of these procedures suffer from tedious synthetic paths, harsh reaction conditions, prolonged reaction time, corrosiveness, toxicity, cost, and catalyst reusability. As a result of this simple, environment friendly, and versatile processes are still required. Now-a-days, multicomponent reaction protocol became a tool, which has been approved as an advanced tool for renewable and sustainable synthetic organic chemistry. The efficiency of catalytic techniques used in multicomponent reaction protocol has made it easier to gain access to novel libraries of organic compounds with great biological potential.

In this concern, we have introduced a new and greener route for the one-pot synthesis of 2,4,5-triaryl substituted imidazole derivatives from benzil, aldehyde, and ammonium acetate under solvent-free conditions at 70 °C with a high product yield in a shorter period of time with easy and simple reaction workup. The presently synthesized catalysts showed significant catalytic activity in these derivative syntheses.

2. Experimental section

2.1. Materials and methods

All the chemicals and solvents were purchased by Sigma-Aldrich, Merck and Molychem companies of high purity and used directly in the reaction protocol without further purification. The powder X-ray diffraction technique was utilized with well-calibrated instrument a Bruker D8-advanced diffractometer with Cu Kα radiation ranges from 5° and 60° (2θ values). The FTIR spectra were obtained on a Shimadzu FTIR 8300 spectrophotometer. The elemental composition was carried *via* objects 8724. The specific surface area and pore volume were determined on Quantachrome instruments version 3.01 with Brunauer–Emmett–Teller method. Morphology of the Lewis acid catalyst samples was analyzed by FE-SEM on instrument Nova Nano SEM NPEP303 and high-resolution transmission electron microscopy images were captured using an instrument JEOL JEM 2100 Plus microscope. All the organic transformations progress were preliminary monitored by thin-layer chromatography (TLC). The ^{1}H NMR spectra (400 MHz) and ^{13}C NMR spectra (100 MHz) were run on a Bruker (400 MHz) spectrometer using DMSO-d6 solvent and tetramethyl silane (TMS) as an internal reference. All reactions were carried out under reflux conditions using a laboratory equipment oil bath and magnetic stirrer. Melting points were recorded on the digital melting point apparatus.

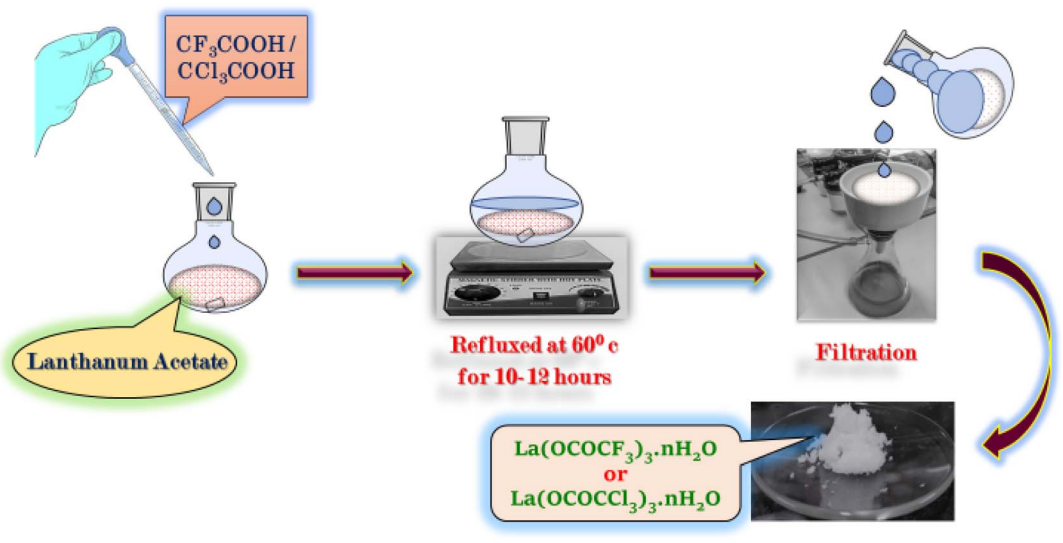

Scheme 1 Synthesis of lanthanum trifluoroacetate ($La(OCOCF_3)_3 \cdot nH_2O$) and trichloroacetate ($La(OCOCCl_3)_3 \cdot nH_2O$).

2.2. Synthesis of lanthanum trifluoroacetate ($La(OCOCF_3)_3 \cdot nH_2O$) and trichloroacetate ($La(OCOCCl_3)_3 \cdot nH_2O$)

The lanthanum trifluoroacetate and trichloroacetate were prepared by new and slight modification in Fujihara method[30] by direct reaction between lanthanum acetate (1 g) with a slightly excess amount of trifluoroacetic acid/trichloroacetic acid (4 g) respectively in 1 : 3 equivalence ratio in 100 ml round bottom flask. The reaction mixture was refluxed at 60 °C for 10–12 hours. The white product obtained in the reaction was further separated *via* vacuum filtration to remove unreacted acid and side product acetic acid from the reaction mixture. The product was washed with *n*-hexane and dried in an oven at 50 °C for 2–3 hours (Scheme 1).

2.3. Synthesis of silica supported lanthanum trifluoroacetate ($La(OCOCF_3)_3 \cdot nH_2O/SiO_2$) and trichloroacetate ($La(OCOCF_3)_3 \cdot nH_2O/SiO_2$) Lewis acid catalyst

The silica supported lanthanum trifluoroacetate and trichloroacetate Lewis acid catalyst was prepared according to literature known procedures[31] with slight modifications. The lanthanum trifluoroacetate/trichloroacetate (1 g) was added to methanol solvent (50 ml) in 100 ml round bottom flask connected with a reflux condenser and a magnetic stirrer bar. The supporting material Kieselgel K100 or silica gel (10 g), was adding up and the resultant slurry of the reaction mixture was well stirred at room temperature for 7–8 hours. The solvent was then evaporated in a sonicator at 70 °C for 1 hour. Finally solid porous form of catalyst was kept in a vacuum desiccator for 2–3 hours to obtain its anhydrous form (Scheme 2).

2.4. General procedure for synthesis of 2,4,5-triarylimidazole derivatives (4a–l)

A mixture of benzil (1 mmol), benzaldehyde (1 mmol), ammonium acetate (3 mmol) and silica supported lanthanum trifluoroacetate catalyst (0.04 g) were stirred in oil bath at 70 °C for 14 minutes under solvent-free condition. The progress of reaction was supervised by thin layer chromatography technique (TLC). The reaction mixture was diluted with hot ethanol (15 ml) once the reaction was completed, and it was then filtered to separate the catalyst. Further, the filtrate of reaction mixture was poured into crushed ice to obtain crude solid product which was filtered and recrystallized by using hot ethanol to get a pure crystal of product. The recovered catalyst was washed with ethanol and dried in an vacuum desiccator for 2–3 hours for further reuse.

3. Result and discussion

3.1. Catalyst characterization

3.1.1. FTIR spectroscopic analysis. FTIR spectroscopy was primarily employed to confirm the successful functionalization of lanthanum trifluoroacetate, lanthanum trichloroacetate, silica supported lanthanum trifluoroacetate and trichloroacetate catalysts (Fig. 1).

The FTIR spectra of synthesized catalysts exhibited five characteristic frequencies. The unsupported lanthanum trifluoroacetate and trichloroacetate have FTIR spectrum at 1633 and 1622 cm^{-1} is associated with a CO_2 asymmetric vibration and band appears at 1462, 1452 cm^{-1} represent, CO_2 symmetric vibration. While, silica supported lanthanum trifluoroacetate and trichloroacetate shows CO_2 asymmetric vibration band at 1658, 1645 cm^{-1}. This modification in higher vibrational value in silica supported catalyst is the result of interaction of silica and lanthanum trifluoroacetate and trichloroacetate. Another characteristics doublet spectrum at 1165, 1138 and 1198 cm^{-1} assigned to C–F, C–Cl and C–O bond vibrations of the trifluoroacetate or trichloroacetate groups, while bands in the 850 and 835 cm^{-1} indicate $\delta asCF_3$ and $\delta asCCl_3$.[32] Moreover, FTIR spectrum of silica-supported catalyst showed lower shift and observed new sharp additional bands appears at 1082 cm^{-1} and

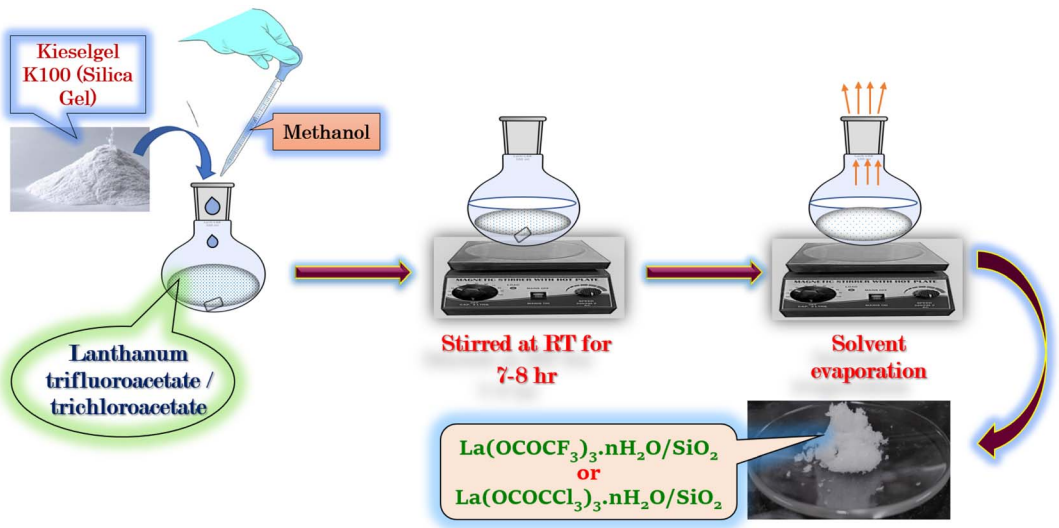

Scheme 2 Silica supported lanthanum trifluoroacetate ($La(OCOCF_3)_3 \cdot nH_2O/SiO_2$) and trichloroacetate ($La(OCOCCl_3)_3 \cdot nH_2O/SiO_2$) Lewis acid catalyst.

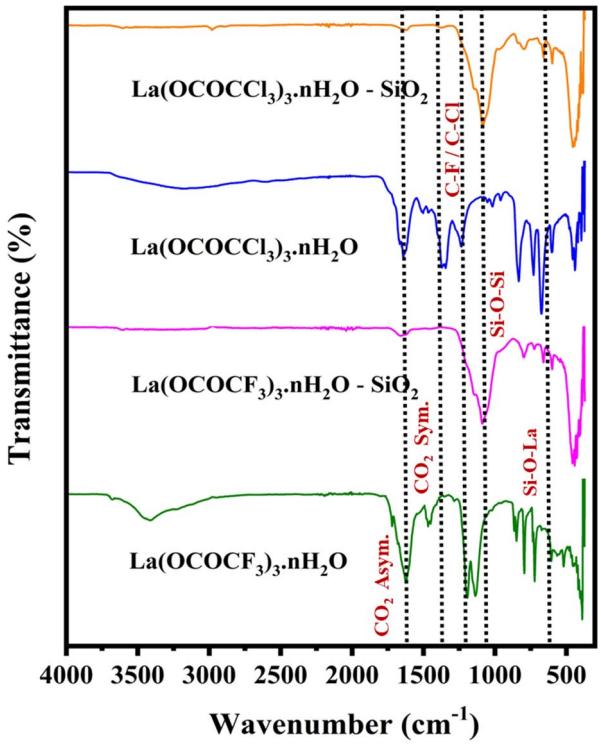

Fig. 1 FT-IR analysis of lanthanum trifluoroacetate, silica supported lanthanum trifluoroacetate, lanthanum trichloroacetate and silica supported lanthanum trichloroacetate composites.

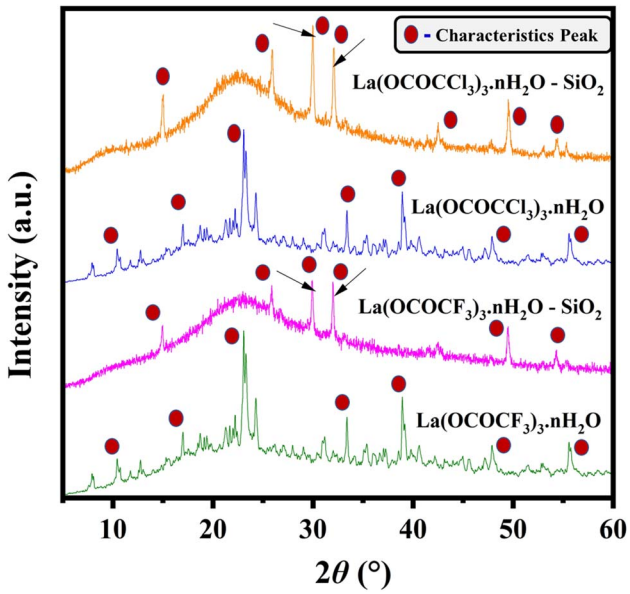

Fig. 2 XRD analysis of lanthanum trifluoroacetate, silica supported lanthanum trifluoroacetate, lanthanum trichloroacetate and silica supported lanthanum trichloroacetate composites.

663 cm^{-1} assigned to Si–O–Si & La–O–Si bond vibrations, attribute more clear confirmation of the successful functionalization and strong electrostatic interaction of lanthanum trifluoroacetate and trichloroacetate with the mesoporous silica support material. The above FTIR results reflect the successful functionalization of silica-supported catalysts having Lewis acidic sites which are actively involved in the synthesis of 2,4,5-triarylimidazoles.

3.1.2. XRD analysis. The fine dispersion of lanthanum trifluoroacetate and trichloroacetate on silica support was confirmed by XRD spectral analysis. Fig. 2 represent the XRD patterns of lanthanum trifluoroacetate ($La(OCOCF_3)_3 \cdot nH_2O$), silica supported lanthanum trifluoroacetate ($La(OCOCF_3)_3 \cdot nH_2O/SiO_2$), lanthanum trichloroacetate ($La(OCOCCl_3)_3 \cdot nH_2O$) and silica supported lanthanum trichloroacetate ($La(OCOCCl_3)_3 \cdot nH_2O/SiO_2$) composites. Unsupported lanthanum trifluoroacetate and trichloroacetate show characteristics diffraction peaks mainly includes 2θ value = 10°, 16°, 23°, 33°, 38°, 47°, 55°.[32,33]

Moreover, silica supported lanthanum trifluoroacetate and trichloroacetate shows modified and prominent intense characteristics diffraction peaks at 2θ = 14°, 25°, 29°, 32°, and 49°, 54°. These results provide clear evidence that lanthanum trifluoroacetate and trichloroacetate were finely dispersed on the silica supported material in the $La(OCOCF_3)_3 \cdot nH_2O$/silica and $La(OCOCCl_3)_3 \cdot nH_2O$/silica catalysts. The broad humped diffraction peaks observed in silica supported lanthanum trifluoroacetate and trichloroacetate catalysts compared to the sharp diffraction peaks in unsupported lanthanum trifluoroacetate and trichloroacetate clearly indicate the disturbance in original crystallinity of catalysts. This change in crystallinity of silica supported catalyst is caused by the strong electrostatic interaction of lanthanum trifluoroacetate and trichloroacetate with the silica support material, which converts the supported catalyst to amorphous nature.[34]

3.1.3. SEM-TEM analysis. The surface morphology and texture of synthesized Lewis acid catalysts were investigated using SEM (Fig. 3a–d) and TEM (Fig. 3e and f) analysis. The Fig. 3a and b indicate irregularly spherical shaped particles with soft and smooth surface for unsupported lanthanum trifluoroacetate and trichloroacetate samples. The SEM images of silica supported lanthanum trifluoroacetate and trichloroacetate are shown in Fig. 3c and d respectively. These images clearly shows that the surface morphology of the supported catalyst is relatively similar to that of unsupported lanthanum trifluoroacetate and trichloroacetate samples. The unchanged surface morphology of the catalysts confirmed that lanthanum trifluoroacetate and trichloroacetate were finely distributed into the mesoporous silica material pores. Further, no separate crystallites of the bulk phase of lanthanum trifluoroacetate and trichloroacetate were observed in silica supported lanthanum trifluoroacetate and trichloroacetate catalysts respectively.

The TEM images of unsupported lanthanum trifluoroacetate and trichloroacetate (Fig. 3e and f) shows that most of the specifically arranged fine particles covered with dark colour. While, the TEM images of silica supported lanthanum trifluoroacetate and trichloroacetate (Fig. 3g and h) indicates proper layered dark colour fine particles on another surface layer of supporting material. This provides strong evidence for uniform dispersion of lanthanum trifluoroacetate and

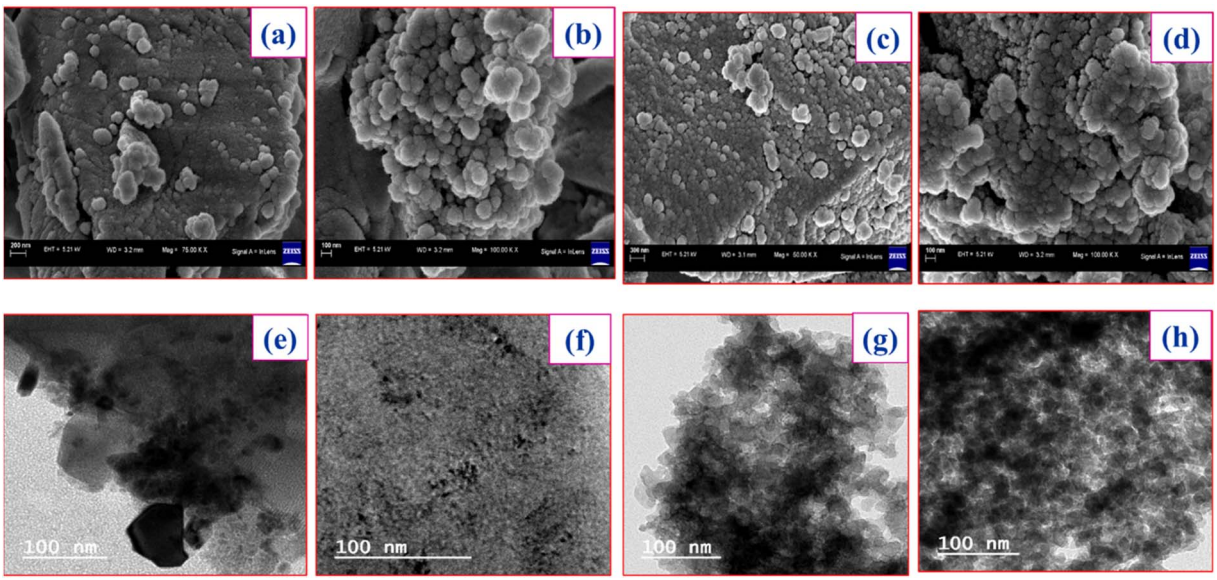

Fig. 3 FE-SEM images of (a) lanthanum trifluoroacetate (b) lanthanum trichloroacetate (c) silica supported lanthanum trifluoroacetate (d) silica supported lanthanum trichloroacetate and HR-TEM images of (e) lanthanum trifluoroacetate (f) lanthanum trichloroacetate (g) silica supported lanthanum trifluoroacetate (h) silica supported lanthanum trichloroacetate.

trichloroacetate inside the mesoporous pores of silica support material.

3.1.4. EDX analysis and mapping images. The chemical constitution of lanthanum trifluoroacetate, silica supported lanthanum trifluoroacetate, lanthanum trichloroacetate and silica supported lanthanum trichloroacetate are confirmed by EDX spectral analysis represented in (Fig. 4). The EDX spectral study of newly synthesized lanthanum trifluoroacetate ($La(OCOCF_3)_3 \cdot nH_2O$) confirm the presence of La, O, C, and F elements (Fig. 4a), while lanthanum trichloroacetate ($La(OCOCCl_3)_3 \cdot nH_2O$) confirm the presence of La, O, C, and Cl elements (Fig. 4c).

Moreover, the EDX results of silica supported lanthanum trifluoroacetate ($La(OCOCF_3)_3 \cdot nH_2O/SiO_2$) showed the presence of La, O, C, and F elements of $La(OCOCF_3)_3 \cdot nH_2O$ and Si, and O of silica (Fig. 4b), while silica supported lanthanum trichloroacetate ($La(OCOCCl_3)_3 \cdot nH_2O/SiO_2$) showed the presence of La, O, C, and Cl elements of $La(OCOCCl_3)_3 \cdot nH_2O$ and Si, and O of silica (Fig. 4d), which strongly indicates the successful formation of silica supported lanthanum trifluoroacetate and trichloroacetate Lewis acid catalysts. The results of EDX elemental image mapping shown in (Fig. 4e and f), revealed the atomic percentage of La, O, C, F, Cl, Si, and O in the synthesized catalysts.

Further, EDX mapping images provides additional validation or confirmation for a uniform distribution of La, O, C, and F in the desired lanthanum trifluoroacetate ($La(OCOCF_3)_3 \cdot nH_2O$) catalyst system (Fig. 4a), while La, O, C, and Cl in the lanthanum trichloroacetate ($La(OCOCCl_3)_3 \cdot nH_2O$) catalyst system (Fig. 4c). The elemental mapping of Fig. 4b and d represents the construction of a finely dispersed blended material of La, O, C, F, Cl, Si, and O in the synthesized silica supported lanthanum trifluoroacetate ($La(OCOCF_3)_3 \cdot nH_2O/SiO_2$) and lanthanum trichloroacetate ($La(OCOCCl_3)_3 \cdot nH_2O/SiO_2$) Lewis acid catalyst that is in moral agreement with FT-IR, XRD and SEM-TEM spectral results.

3.1.5. BET analysis. The specific surface area is a significant indicator of a catalyst. The BET technique was used to measure the specific surface area, pore diameter, and pore volume of the synthesized supported and unsupported Lewis acid catalysts. The specific surface area of the lanthanum trifluoroacetate ($La(OCOCF_3)_3 \cdot nH_2O$), lanthanum trichloroacetate ($La(OCOCCl_3)_3 \cdot nH_2O$), silica supported lanthanum trifluoroacetate ($La(OCOCF_3)_3 \cdot nH_2O/SiO_2$) and lanthanum trichloroacetate ($La(OCOCCl_3)_3 \cdot nH_2O/SiO_2$) Lewis acid catalysts were 21.278, 19.198, 113.545 and 45.001 $m^2\ g^{-1}$, respectively (Table 1). The porosity of these catalyst samples was analysed by the nitrogen adsorption–desorption measurement.

The nitrogen adsorption–desorption isotherm is of type V in nature according to the IUPAC classification. The bulk unsupported lanthanum trifluoroacetate, lanthanum trichloroacetate, silica supported lanthanum trifluoroacetate and trichloroacetate Lewis acid catalysts exhibit a well expressed H_3 hysteresis loop (Fig. 5a–d), in the order of 0.4–1.0P/P^0 at high relative pressure, which is most common for mesoporous materials.[35] As represented in Table 1, the average pore diameter of the lanthanum trifluoroacetate, lanthanum trichloroacetate, silica supported lanthanum trifluoroacetate and lanthanum trichloroacetate catalyst were 9.0766, 7.5292, 11.102 and 11.958 nm respectively. Also, total pore volume (0.0436–0.3151 $cm^3\ g^{-1}$) of the catalysts was calculated using the BJH method (see Fig. 5a–d).

The BET study proved that the surface area of lanthanum trifluoroacetate and trichloroacetate catalysts supported by silica was marginally greater than that of the same catalysts without support. The main cause of this might be the

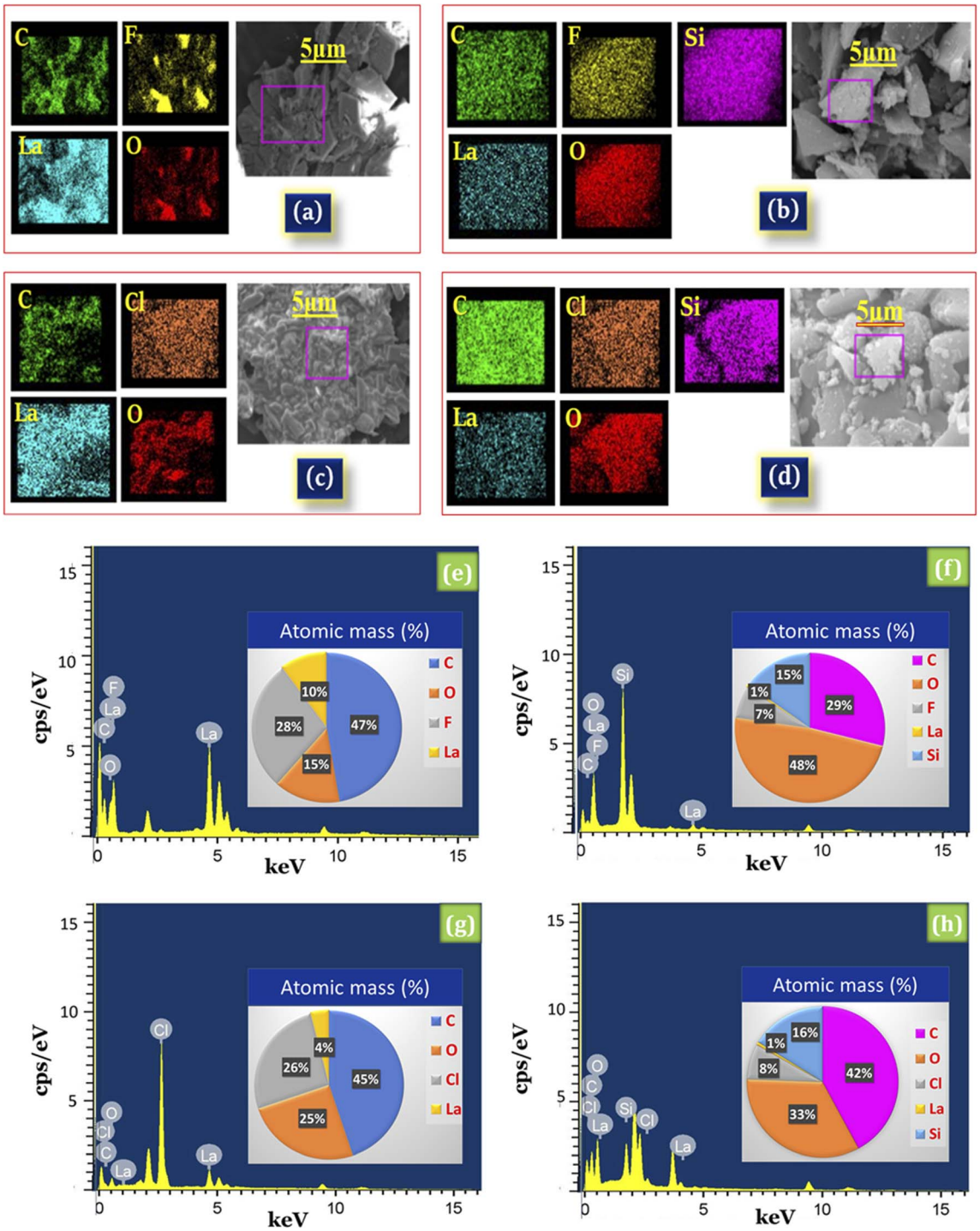

Fig. 4 Elemental mapping images of (a) lanthanum trifluoroacetate (b) silica supported lanthanum trifluoroacetate (c) lanthanum trichloroacetate (d) silica supported lanthanum trichloroacetate and EDX spectra for atomic percentage of (e) lanthanum trifluoroacetate (f) silica supported lanthanum trifluoroacetate (g) lanthanum trichloroacetate (h) silica supported lanthanum trichloroacetate.

deposition and incorporation of lanthanum trifluoroacetate or trichloroacetate into the pores of the mesoporous silica support material. The increased surface area, average pore diameter and total pore volume of silica supported Lewis acid catalysts may become one of the key features in enhancing catalytic performance.

3.1.6. TGA analysis. Thermogravimetric analysis (TGA) was used to determine the thermal stability of unsupported and silica-supported lanthanum trifluoroacetate and trichloroacetate Lewis acid catalyst. The first characteristic TGA curves of all synthesized Lewis acid catalysts (from temperature range 74 °C to 140 °C) are associated with the loss of water

Table 1 BET analysis of the Lewis acid catalyst series

Entry	Catalyst sample	S_{BET} ($m^2\ g^{-1}$)	D_{pore} (nm)	V_{pore} ($cm^3\ g^{-1}$)
1	$La(OCOCF_3)_3 \cdot nH_2O$	21.278	9.0766	0.0436
2	$La(OCOCCl_3)_3 \cdot nH_2O$	19.198	7.5292	0.0361
3	$La(OCOCF_3)_3 \cdot nH_2O/SiO_2$	113.545	11.102	0.3151
4	$La(OCOCCl_3)_3 \cdot nH_2O/SiO_2$	45.001	11.958	0.1345

molecules as shown in Fig. 6. In unsupported lanthanum trifluoroacetate and trichloroacetate catalysts, the second characteristic curve (from temperature range 184 °C to 252 °C) with minimum mass loss of 26 and 44% respectively, was assumed to be due to a partial loss of trifluoroacetate and trichloroacetate group of the anhydrous Lewis acid. While third curve (from temperature range 259 °C to 310 °C) with maximum mass loss of 65 and 70% respectively, was associated due to a complete loss of trifluoroacetate and trichloroacetate group of the anhydrous Lewis acid with the formation of LaF_3 and $LaCl_3$ decomposition product.[32,33]

In the TGA of silica supported lanthanum trifluoroacetate and trichloroacetate catalysts, the second characteristic curves (from temperature range 198 °C to 271 °C) with minimum mass loss of 14 and 12% respectively, were assumed to be due to a partial loss of trifluoroacetate and trichloroacetate group of the anhydrous Lewis acid. While third curve (from temperature range 276 °C to 326 °C) with maximum mass loss of 19 and 15% respectively, were associated due to a complete loss of trifluoroacetate and trichloroacetate group of the anhydrous Lewis acid.

Herein, TGA study of these Lewis acid catalyst provides strong confirmation that the thermal stability of supported Lewis acid catalysts were increased than that of the catalyst alone. This must be due to the interaction between silica and bulk lanthanum trifluoroacetate or trichloroacetate catalyst. These advancements in thermal stability of the supported catalyst leads to moderate a range of temperatures over which it can be used without a significant loss in catalytic activity, achieving reactions at higher temperatures as well as preventing sintering of metal in order to prolong life of the catalyst.

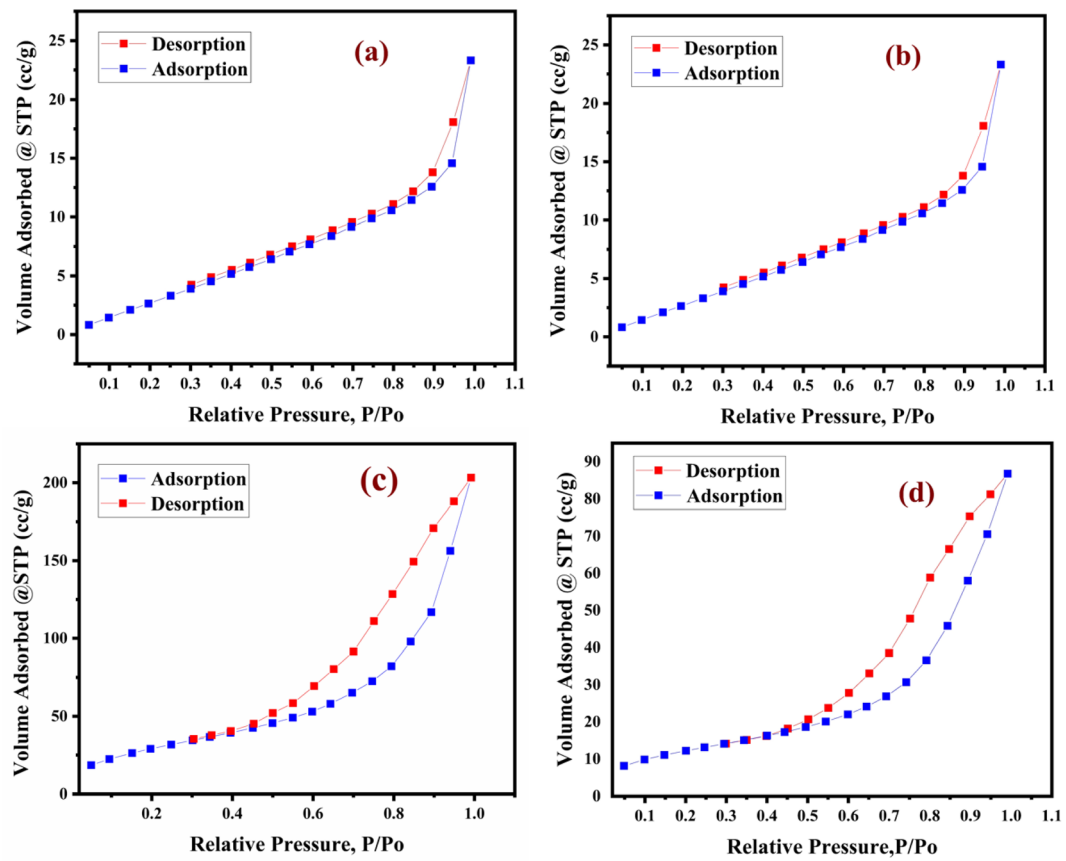

Fig. 5 Nitrogen adsorption–desorption isotherms of (a) lanthanum trifluoroacetate (b) lanthanum trichloroacetate (c) silica supported lanthanum trifluoroacetate (d) silica supported lanthanum trichloroacetate.

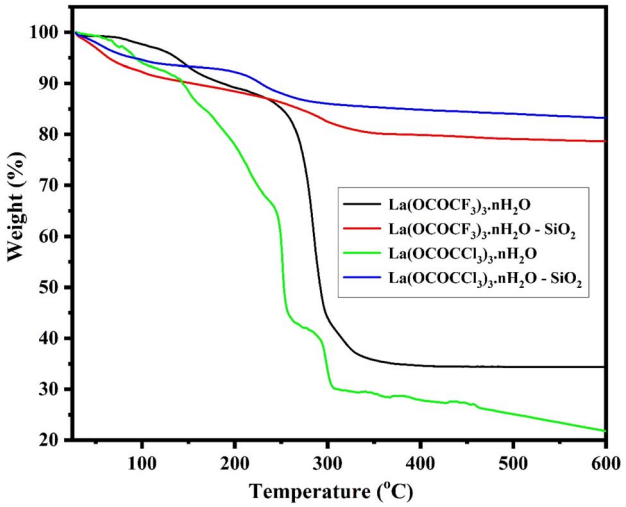

Fig. 6 TGA analysis of lanthanum trifluoroacetate, silica supported lanthanum trifluoroacetate, lanthanum trichloroacetate and silica supported lanthanum trichloroacetate composites.

3.2. Catalytic activity of silica supported Lewis acid catalysts for the synthesis of 2,4,5-trisubstituted arylimidazole derivatives

The first focus of our studies was to evaluate the efficiency of synthesized Lewis acid catalysts and optimization of the best reaction conditions for the one-pot synthesis of 2,4,5-triarylimidazole derivatives. Benzaldehyde (1 mmol), benzil (1 mmol) and ammonium acetate (3 mmol) were chosen as substrates for the model reaction (Scheme 3).

In order to evaluate the efficiency of synthesized Lewis acid catalysts, the model reaction was carried *via* unsupported Lewis acid catalysts $La(OCOCF_3)_3 \cdot nH_2O$ & $La(OCOCCl_3)_3 \cdot nH_2O$ and silica supported Lewis acid catalysts $La(OCOCF_3)_3 \cdot nH_2O/SiO_2$ & $La(OCOCCl_3)_3 \cdot nH_2O/SiO_2$ under solvent free condition (Table 2). The unsupported Lewis acid catalysts show lesser catalytic efficiency in respect of reaction time period and product yields as compared to similar catalysts with silica support. It was found that product yield and reaction time period was improved a lot by the silica supported Lewis acid catalysts. While, pure silica supporting material shows incredibly poor catalytic activity in terms of the expected product yield and reaction time period (Table 2, entry 5).

Table 2 Comparative study of catalytic activity/efficiency of synthesized Lewis acid catalysts in 2,4,5-trisubstituted arylimidazole derivative synthesis (**4a**)[a]

Entry	Catalyst sample	Time[b] (min)	Yield[c] (%)
1	$La(OCOCF_3)_3 \cdot nH_2O$	45	71
2	$La(OCOCCl_3)_3 \cdot nH_2O$	48	68
3	**$La(OCOCF_3)_3 \cdot nH_2O/SiO_2$**	**14**	**96**
4	**$La(OCOCCl_3)_3 \cdot nH_2O/SiO_2$**	**17**	**94**
5	Kieselgel K100 (silica gel)	220	41

[a] Reaction conditions: benzaldehyde (1 mmol), benzil (1 mmol), ammonium acetate (3 mmol) and synthesized Lewis acid catalysts. [b] Reaction progress monitored by TLC. [c] Isolated yields.

This indicates that silica supported Lewis acid catalysts $La(OCOCF_3)_3 \cdot nH_2O/SiO_2$ & $La(OCOCCl_3)_3 \cdot nH_2O/SiO_2$ shows very high catalytic activity/efficiency. The increase in activity of the silica supported Lewis acid catalysts were due to high dispersion of lanthanum trifluoroacetate or trichloroacetate Lewis acid catalyst on silica support. As a result, it would have more surface area and active Lewis and Brønsted sites than the unsupported Lewis acid catalysts $La(OCOCF_3)_3 \cdot nH_2O$ & $La(OCOCCl_3)_3 \cdot nH_2O$. Moreover, the comparative study of catalytic efficiency of silica supported lanthanum trifluoroacetate ($La(OCOCF_3)_3 \cdot nH_2O/SiO_2$) and lanthanum trichloroacetate ($La(OCOCCl_3)_3 \cdot nH_2O/SiO_2$) Lewis acid catalysts were also performed, which clearly indicates that silica supported lanthanum trifluoroacetate shows higher catalytic activity/efficiency than silica supported lanthanum trichloroacetate.

Further, we have monitored the model reaction under many conditions, such as the various solvents, temperature range and catalyst amount, in order to determine the ideal reaction parameters for this multicomponent reaction in presence of synthesized silica supported Lewis acid catalysts. The different range of solvents (polar and non-polar solvent) were utilized to examine the catalytic activity of the synthesized silica supported lanthanum trifluoroacetate and trichloroacetate Lewis acid catalysts. It was observed that the solvent-free environment produced the best results in terms of reaction time and product yield (Table 3). This must be because in solvent-free conditions, the larger availability of the reactant molecules allows for easy access to the active sites through the pores of the catalyst, and this porous structure produces the best results compared to in a solvent. In a solvent, the presence of solvent molecules

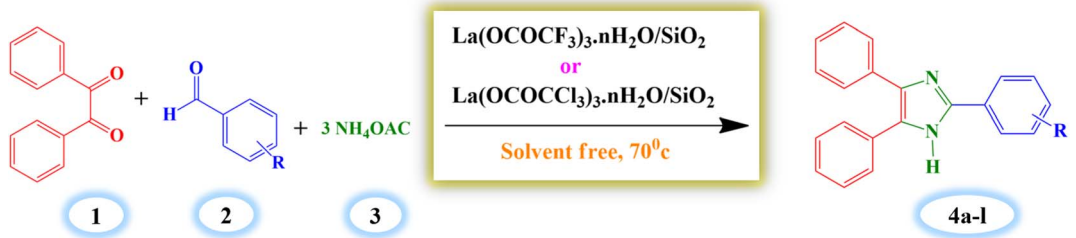

Scheme 3 Silica supported lanthanum trifluoroacetate and trichloroacetate Lewis acid catalysed synthesis of 2,4,5 triaryl imidazole.

Table 3 Optimization of solvents and comparison of temperature for silica supported lanthanum trifluoroacetate ($La(OCOCF_3)_3 \cdot nH_2O/SiO_2$) and lanthanum trichloroacetate ($La(OCOCCl_3)_3 \cdot nH_2O/SiO_2$) Lewis acid catalysts in the synthesis of 2,4,5-trisubstituted arylimidazole derivatives (**4a**)[a]

Entry	Solvents	Reaction condition (temp.)	Time[b] (min)		Yield[c] (%)	
			A Catalyst	**B Catalyst**	**A Catalyst**	**B Catalyst**
1	Water	Reflux	64	72	70	68
2	Ethanol	Reflux	38	40	90	89
3	DMF	Reflux	46	48	76	72
4	THF	Reflux	43	47	81	78
5	Acetonitrile	Reflux	68	74	67	62
6	Chloroform	Reflux	65	70	69	67
7	Toluene	Reflux	84	90	65	62
8	Solvent free	Reflux	17	22	85	83
9	Solvent free	50 °C	20	24	78	74
10	Solvent free	60 °C	14	17	85	81
11	**Solvent free**	**70 °C**	**14**	**17**	**96**	**94**
12	Solvent free	80 °C	14	17	96	94
13	Solvent free	90 °C	14	17	96	94

[a] Reaction conditions: benzaldehyde (1 mmol), benzil (1 mmol), ammonium acetate (3 mmol) and (**A Catalyst**) – silica supported lanthanum trifluoroacetate or (**B Catalyst**) – silica supported lanthanum trichloroacetate. [b] Reaction progress monitored by TLC. [c] Isolated yields.

reduces the availability of reactant molecules, which lowers the yield of the product in comparison to a solvent-free reaction. Since solvent free reaction condition provided the best results in terms of reaction time and product yield, temperature optimization was also carried out at the solvent free condition, in order to examine the best reaction temperature for the overall synthesis of the 2,4,5-trisubstituted arylimidazole derivatives listed in Table 3. The reaction time and product yield improved gradually and steadily as the temperature range increased from 50 to 70 °C. The results show that 70 °C is the ideal reaction temperature for this one-pot, solvent-free multicomponent synthesis. Furthermore, the reaction progress time and product yield were not significantly affected by the temperature increase above 70 °C.

The determination of appropriate and stoichiometric amount of the catalyst for the reaction is another crucial factor for reaction effectiveness. To find appropriate amount of catalyst required, the model reaction was carried out under solvent free condition in the presence of different amounts (0.01, 0.02, 0.03, 0.04, 0.05, and 0.06 g) of both silica supported lanthanum trifluoroacetate and trichloroacetate lewis acid catalysts and obtained results are summarized in Table 4.

When the amount of these Lewis acid catalysts increases progressively, product yield also increases (Table 4, entries 1–6). The obtained results demonstrate that 0.04 g amount of both silica supported lanthanum trifluoroacetate and trichloroacetate Lewis acid catalysts gave 96% and 94% yield of product respectively at 70 °C temperature (Table 4, entry 4). An additional increase in the amount (0.05, and 0.06 g) of these Lewis acid catalysts does not increase yield of the product (Table 4, entry 5, 6). This could be as a result of the catalyst reaching its maximum conversion efficiency.

Finally, the 2,4,5-trisubstituted arylimidazole derivatives (**4a–l**) were synthesized employing the catalytic system under the optimum reaction conditions, and excellent results were achieved, which are well described in Table 5. However, out of

Table 4 Optimization of the amount of silica supported Lewis acid catalysts and comparison of reaction time and product yield (%) for the synthesis of (**4a**)[a] under solvent free condition

Entry	Amount of catalyst (g)	Reaction condition (temp.)	Time[b] (min)		Yield[c] (%)	
			A Catalyst	**B Catalyst**	**A Catalyst**	**B Catalyst**
1	0.01	70 °C	14	17	67	66
2	0.02	70 °C	14	17	74	71
3	0.03	70 °C	14	17	85	81
4	**0.04**	**70 °C**	**14**	**17**	**96**	**94**
5	0.05	70 °C	14	17	96	94
6	0.06	70 °C	14	17	96	94

[a] Reaction conditions: benzaldehyde (1 mmol), benzil (1 mmol), ammonium acetate (3 mmol) and (**A Catalyst**) – silica supported lanthanum trifluoroacetate or (**B Catalyst**) – silica supported lanthanum trichloroacetate. [b] Reaction progress monitored by TLC. [c] Isolated yields.

Table 5 Silica supported lanthanum trifluoroacetate ($La(OCOCF_3)_3 \cdot nH_2O/SiO_2$) and lanthanum trichloroacetate ($La(OCOCCl_3)_3 \cdot nH_2O/SiO_2$) Lewis acid catalysed synthesis of 2,4,5-trisubstituted arylimidazole derivatives (**4a–l**)[a]

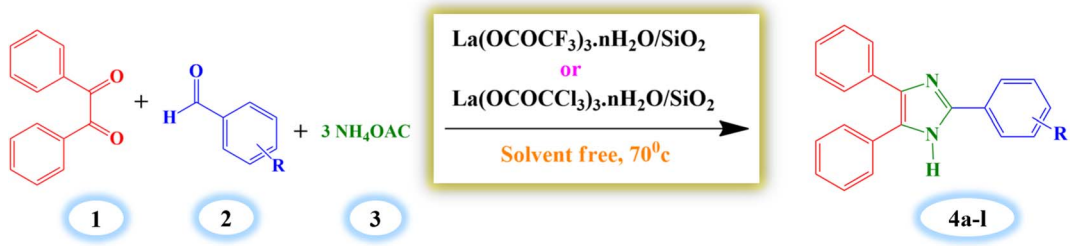

Entry	Substituent 'R'	Time[b] (min)		Yield[c] (%)		M.P. (°C) observed	M.P. (°C) reported
		A Catalyst	**B Catalyst**	**A Catalyst**	**B Catalyst**		
4a	H	14	17	96	94	269–270	270–272 [37]
4b	4-OMe	15	18	96	93	229–231	231–232 [38]
4c	4-Me	16	18	95	93	228–230	231–232 [39]
4d	4-Br	14	17	95	92	257–260	254–256 [40]
4e	4-F	14	19	96	94	188–190	190 [41]
4f	4-Cl	14	17	96	92	261–263	257–260 [42]
4g	4-NO_2	16	20	92	90	242–245	241–242 [43]
4h	2-Me	16	19	95	92	253–255	255–258 [44]
4i	2-Cl	15	18	95	93	189–192	188 [45]
4j	3-Br	16	17	93	91	293–295	298–300 [45]
4k	4-OH	14	18	96	93	255–258	254–256 [46]
4l	3-OH	15	19	93	91	259–261	260–261 [47]

[a] Reaction conditions: benzaldehyde (1 mmol), benzil (1 mmol), ammonium acetate (3 mmol) and (**A Catalyst**) – silica supported lanthanum trifluoroacetate or (**B Catalyst**) – silica supported lanthanum trichloroacetate. [b] Reaction progress monitored by TLC. [c] Isolated yields.

this silica supported lanthanum trifluoroacetate and trichloroacetate Lewis acid catalysts, silica supported lanthanum trifluoroacetate shows more catalytic activity compared to silica supported lanthanum trichloroacetate in respect of all optimization parameters and arylimidazole derivatives (**4a–l**) synthesis. Actually, this is due to the fact that high electronegative fluorine atoms increase the acidity of Lewis acid catalyst by its more withdrawing nature as compared to chlorine atoms.

A comparative study, which includes silica supported lanthanum trifluoroacetate and trichloroacetate Lewis acid as a catalyst was performed for the synthesis of 2,4,5-trisubstituted arylimidazole derivatives with various catalysts reported in the literature (see Table 6). In comparison to silica supported lanthanum trifluoroacetate and trichloroacetate Lewis acid catalysts in solvent-free systems, reactions with other different catalysts required a higher amount of catalyst and longer reaction time period which produces a low yield of the desired product also. As a result, the present Lewis acid catalyst promoted the reactions more successfully than the other catalysts and should become one of the best options for choosing an

Table 6 Comparison of the current catalysts with reported catalysts for the synthesis of 2,4,5-trisubstituted arylimidazole derivatives (**4a**)[a]

Entry	Catalyst	Conditions	Time[b] (min)	Yield[c] (%)
1	Without catalyst	Reflux	720	NR
2	CH_3COOH	Reflux	120	40 [48]
3	Montmorillonite K10	EtOH, reflux	90	70 [40]
4	Polymer–$ZnCl_2$	EtOH, reflux	240	96 [49]
5	Nano-$SnCl_4.SiO_2$	Solvent-free/130 °C	120	96 [50]
6	Ceric ammonium nitrate	EtOH, reflux	360	75 [51]
7	$Yb(OTf)_3$	Acetic acid, reflux	160	92 [52]
8	$Y(TFA)_3$	Reflux/100 °C	180	95 [53]
9	ZSM-11	Solvent-free/110 °C	30	90 [54]
10	$La(OCOCCl_3)_3 \cdot nH_2O/SiO_2$	Solvent-free, 70 °C	17	94 (this work)
11	$La(OCOCF_3)_3 \cdot nH_2O/SiO_2$	Solvent-free, 70 °C	14	96 (this work)

[a] Reaction conditions: benzaldehyde (1 mmol), benzil (1 mmol), ammonium acetate (3 mmol) and silica supported lanthanum trifluoroacetate or silica supported lanthanum trichloroacetate Lewis acid catalysts. [b] Reaction progress monitored by TLC. [c] Isolated yields.

economically convenient, and environmentally eco-friendly catalyst.

3.3. Proposed plausible structure for active site of silica supported Lewis acid catalyst

The proposed model of active site of silica supported lanthanum trifluoroacetate and trichloroacetate Lewis acid catalysts is well depicted in Fig. 7. These catalysts mainly indicate Lewis acid sites on lanthanum metal which is attached to the mesoporous surface of silica support material. The trifluoroacetate or trichloroacetate group withdraws the electron density from the metal atom (La) which leads to making it electron deficient and developing Lewis acidity. The interaction of trifluoroacetate or trichloroacetate with surface –OH groups of silica bind them on the silica surface without moderating its Lewis acidity. It is well reported that the silica supported lanthanum trifluoroacetate and trichloroacetate solid heterogeneous catalysts mainly includes Lewis acidity, which is actually originated from the loaded lanthanum trifluoroacetate or trichloroacetate.[36]

3.4. Recycling of catalyst

The recyclability of the catalysts is one of the key features of the current methodology. The catalysts were recovered from the reaction mixture by means of simple filtration technique, in such a way that after completion of the reaction, reaction mixture was diluted with hot ethanol and filtered for the separation catalyst. Filtered, solid catalysts were washed with the ethanol/water system (1 : 1). The recovered catalysts were kept under vacuum-oven for 20 min at 80 °C for drying and activation, after which they were weighed and reused in the next run. They were used for five runs without any further treatment in the subsequent reaction. It was found that recovered catalysts almost have consistent activity after several time of use. The present silica supported lanthanum trifluoroacetate and trichloroacetate Lewis acid catalysts even after the fifth recycling, shows 92% and 87% catalytic efficiency respectively (Fig. 9). These studies proved that the current silica supported green Lewis acid catalysts are highly active, efficient and reusable without a considerable loss in catalytic activity. Furthermore,

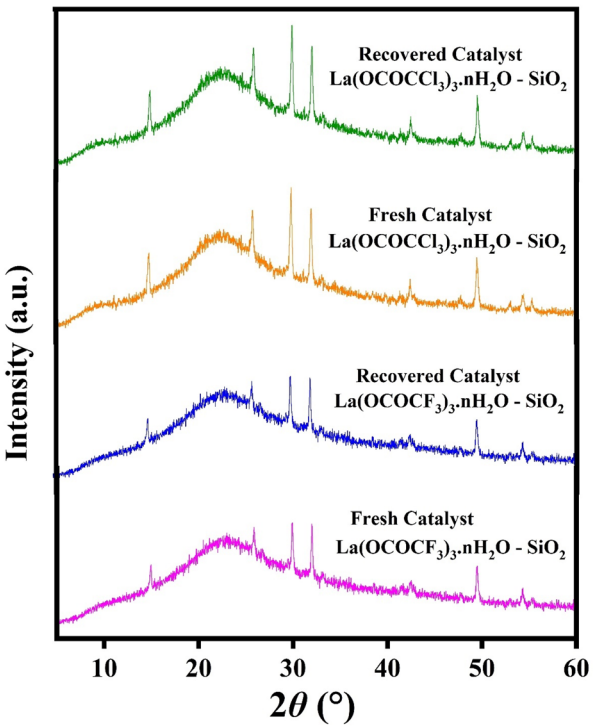

Fig. 8 XRD spectrum of fresh and recovered silica supported lanthanum trifluoroacetate and lanthanum trichloroacetate Lewis acid catalysts.

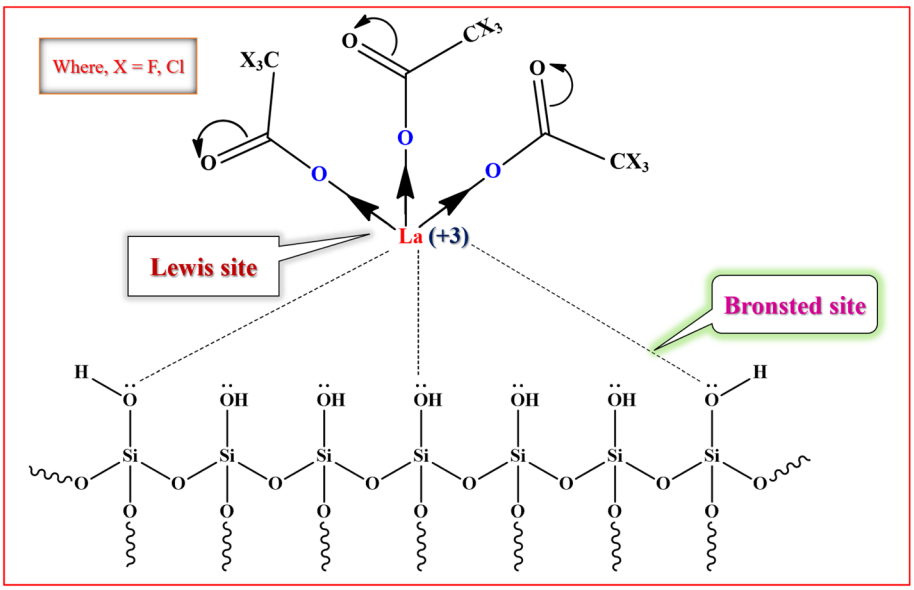

Fig. 7 The proposed model of active site of silica supported lanthanum trifluoroacetate and trichloroacetate Lewis acid catalyst.

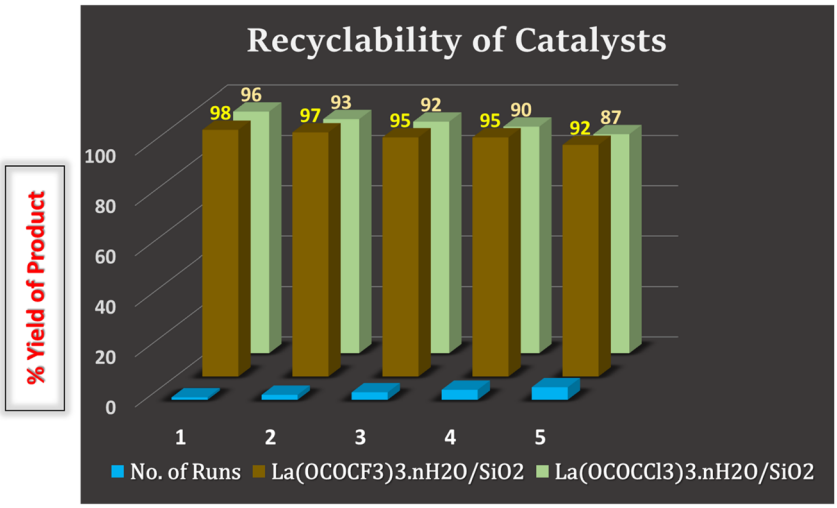

Fig. 9 Recyclability of silica supported lanthanum trifluoroacetate and trichloroacetate Lewis acid catalyst in the synthesis of 2,4,5-triarylimidazole derivatives.

after the fifth cycle, the recycled catalyst was recovered, washed, dried and weighed. This recovered catalyst was then characterized by using powder XRD analysis for its comparative morphological study with fresh catalyst. The diffraction peaks at $2\theta = 14°$, 25°, 29°, 32°, 49°, and 54° of recovered catalysts were exactly identical to the fresh silica supported lanthanum trifluoroacetate and trichloroacetate Lewis acid catalysts (Fig. 8).

3.5. Plausible reaction mechanism

The proposed plausible mechanism for the synthesis of 2,4,5-trisubstituted arylimidazole in presence of currently synthesized green Lewis acid catalyst is well described in Scheme 4, based on literature reports.[13,54] The carbonyl groups of benzil (2) and aromatic aldehydes (1) are activated by silica supported lanthanum trifluoroacetate or trichloroacetate Lewis acid catalyst which leads to an increase in electrophilicity of carbonyl carbon. Then nucleophilic attack of the nitrogen atom of ammonia molecule takes place due to the presence of its free lone pair of electron. The ammonia molecules are generated *in situ* from ammonium acetate which attack on the activated carbonyl carbon of benzil and aromatic aldehydes resulting in the formation of 2-imino-1,2-diphenylethanone intermediate (3) and aryl methanimine intermediate (4). Further, nucleophilic attack of aryl methanimine intermediate (4) to another

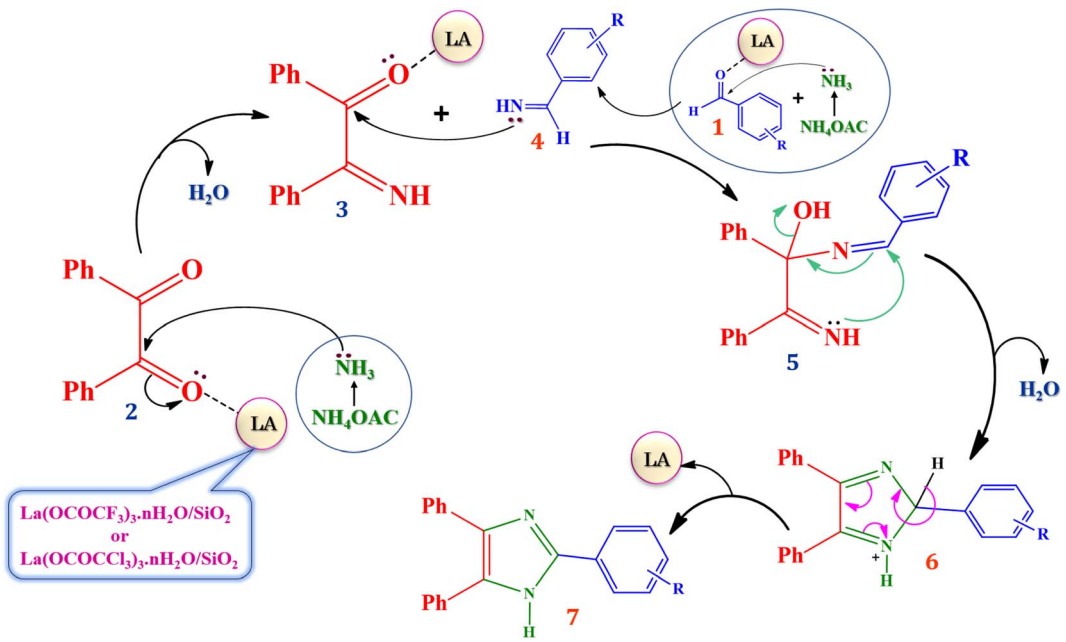

Scheme 4 The proposed reaction mechanism for the formation of 2,4,5-triarylimidazole derivatives in the presence of silica supported lanthanum trifluoroacetate or trichloroacetate Lewis acid catalyst under solvent-free condition.

carbonyl carbon of 2-imino-1,2-diphenylethanone (3) gives 1-(benzylidene amino)-2-imino-1,2-diphenylethanol intermediate (5), which afterward undergoes the cyclization leads to the formation of 2,4,5-triphenyl-2*H*-(1-imidazolium) intermediate (6) further converted into 2,4,5- trisubstituted arylimidazole derivatives by dehydration. However, the catalyst which regenerated after end of each reaction are available for the next reaction cycle.

4. Conclusion

In an overview, we have developed silica supported lanthanum trifluoroacetate and trichloroacetate as water-compatible green Lewis acid catalysts *via* novel, simple, and eco-friendly method. The morphology and properties of synthesized Lewis acid catalysts were studied by FTIR, TGA, XRD, EDX, SEM, TEM and BET analysis techniques. The synthesized catalysts were utilized in the synthesis of 2,4,5-trisubstituted arylimidazole derivatives under solvent-free green reaction protocols. The silica supported lanthanum trifluoroacetate and trichloroacetate catalysts work superiorly in presence of water as well as in organic solvents without loss in their catalytic activity compared to conventional Lewis acid catalysts. However, the best reaction results were found in solvent-free conditions at 70 °C optimum temperature. This reaction protocol has many advantages as being highly efficient with excellent product yield in shorter reaction time, work-up simplicity and no side reactions. The comparative study of catalytic efficiency of these two catalysts was also performed in terms of reaction time, reaction temperature, and influence of different solvents on yield of the product. This clearly indicates that silica supported lanthanum trifluoroacetate shows higher catalytic activity and efficiency than silica supported lanthanum trichloroacetate.

These catalysts offer several remarkable features. They are non-hazardous, water compatible, work superiorly in the different range of solvents under mild reaction conditions with best product yields, easily recovered and reused in reactions. These catalysts were economically valuable as they were synthesized from commercially available cheap starting materials. Moreover, the synthesized silica supported Lewis acid catalysts are non-hygroscopic, moisture insensitive, environment friendly and inexpensive compared to metal triflate Lewis acid catalysts. This will make them one of the best competent alternatives for metal triflate Lewis acid catalysts as well as to the heterogeneous acid catalysts.

Conflicts of interest

The authors declared that there is no conflict of interest in the publication of this research paper.

Acknowledgements

The authors Dnyaneshwar Purushottam Gholap and Prof. M. K. Lande gratefully acknowledge UGC-DST SAP for financial assistance. We are also thankful to the Department of Chemistry, Dr Babasaheb Ambedkar Marathwada University, Aurangabad (MS), India for providing laboratory facilities.

References

1 A. Dhakshinamoorthy, A. Santiago-Portillo, A. M. Asiri and H. Garcia, *ChemCatChem*, 2019, **11**, 899.
2 T. Zhang, *Chem. Sci.*, 2021, **12**, 12529–12545.
3 A. H. Chughtai and others, *Chem. Soc. Rev.*, 2015, **44**, 6804–6849.
4 (*a*) C. M. Friend and B. Xu, *Acc. Chem. Res.*, 2017, **50**, 517–521; (*b*) D. S. Aher, K. R. Khillare, L. D. Chavan and S. G. Shankarwar, *RSC Adv.*, 2021, **11**, 2783–2792; (*c*) D. S. Aher, K. R. Khillare, L. D. Chavan and S. G. Shankarwar, *RSC Adv.*, 2021, **11**, 33980–33989; (*d*) R. G. Jadhav, D. Singh and A. K. Das, *Sustainable Energy Fuels*, 2020, **4**, 1320–1331.
5 W. Chao, Y. Anyuan and D. Wei-Lin, *Appl. Catal., B*, 2014, **160–161**, 730–741.
6 (*a*) L. Lin X. Han, B. Han and S. Yang, *Chem. Soc. Rev.*, 2021, **50**, 11270–11292; (*b*) Q. Yangjian, L. Guangxu, F. Yingjie, S. Wenjie, Y. Eric and L. Wenbin, *J. Am. Chem. Soc.*, 2020, **142**, 1746–1751; (*c*) O. Awogbemi, D. V. Von Kallon and V. S. Aigbodion, *J. Energy Inst.*, 2021, **98**, 244–258.
7 S. Kobayashi, M. Sugira, H. kitagawa, W. William and L. Lam, *Chem. Rev.*, 2002, **120**, 2227–2302.
8 (*a*) M. Hiroyuki, F. Risa, S. Yuhei, M. Kazuhiro and O. Takashi, *Org. Lett.*, 2014, **16**, 2018–2021; (*b*) T. Beisel and G. Manolikakes, *Org. Lett.*, 2013, **15**, 6046–6049; (*c*) G. A. Meshram, S. S. Deshpande, P. A. Wagh and V. A. Vala, *Tetrahedron Lett.*, 2014, **55**, 3557–3560.
9 (*a*) S. Kobayashi, *Synlett*, 1994, **9**, 689–701; (*b*) R. W. Marshman, *Aldrichimica Acta*, 1995, **28**, 77–84; (*c*) S. Kobayashi, *Chem. Lett.*, 1991, **20**, 2187–2190.
10 J. H. Forsberg, V. T. Spaziano, T. M. Balasubramanian, G. K. Liu, S. A. Kinsley, C. A. Duckworth, J. J. Poteruca, P. S. Brown and J. L. Miller, *J. Org. Chem.*, 1987, **52**, 1017–1021.
11 S. Kobayashi and K. Manabe, *Acc. Chem. Res.*, 2002, **35**, 209–217.
12 B. Kumar, K. Smita, B. Kumar and L. Cumbal, *J. Chem. Sci.*, 2014, **126**, 1831–1840.
13 (*a*) D. Song, C. Liu, S. Zhang and G. Luo, *Synth. React. Inorg., Met.-Org., Nano-Met. Chem.*, 2010, **40**, 145–147; (*b*) K. H. Asressu, C. K. Chan and C. C. Wang, *RSC Adv.*, 2021, **11**, 28061–28071.
14 K. N. Tayade, M. Mishra, K. Munusamy and R. S. Somani, *Catal. Sci. Technol.*, 2015, **5**, 2427–2440.
15 (*a*) H. Firouzabadi, N. Iranpoor, A. A. Jafari and M. R. Jafari, *J. Organomet. Chem.*, 2008, **693**, 2711–2714; (*b*) H. Adibi, H. A. Samimi and M. Beygzadeh, *Catal. Commun.*, 2007, **8**, 2119–2124.
16 (*a*) A. Corma and H. Garcıa, *Chem. Rev.*, 2003, **103**, 4307–4366; (*b*) E. B. Mubofu and J. B. F. N. Engberts, *J. Phys. Org. Chem.*, 2004, **17**, 180–186.

17 (*a*) L. D. Luca, *Curr. Med. Chem.*, 2006, **13**, 1–23; (*b*) C. K. Jadhav, A. S. Nipate, A. V. Chate, P. M. Kamble, G. A. Kadam, V. S. Dofe, V. M. Khedkar and C. H. Gill, *J. Chin. Chem. Soc.*, 2021, **68**, 1067–1081.
18 M. Gaba and C. Mohan, *Med. Chem. Res.*, 2016, **25**, 173–210.
19 R. Kreutz, *Vasc. Health Risk Manage.*, 2011, **7**, 183–192.
20 J. G. Hoogerheide and B. E. Wyka, Clotrimazole, *Analytical Profiles of Drug Substances*, 1982, vol. 11, pp. 225–255.
21 M. H. Fisher and A. Lusi, *J. Med. Chem.*, 1972, **15**, 982–985.
22 (*a*) J. Li, T. S. Kaoud, C. Laroche, K. N. Dalby and S. M. Kerwin, *Bioorg. Med. Chem. Lett.*, 2009, **19**, 6293–6297; (*b*) S. Tahlan, S. Kumar and B. Narasimhan, *BMC Chem.*, 2019, **13**, 1–27; (*c*) M. Sánchez-Moreno, F. Gómez-Contreras, P. Navarro, C. Marín, F. Olmo, M. J. R. Yunta, A. M. Sanz, M. J. Rosales, C. Cano and L. Campayo, *J. Med. Chem.*, 2012, **55**, 9900–9913; (*d*) N. Zhao, Y. L. Wang and J. Y. Wang, *J. Chin. Chem. Soc.*, 2005, **52**, 535–538.
23 (*a*) A. V. Chate, S. P. Kamdi, A. N. Bhagat, C. K. Jadhav, A. Nipte, A. P. Sarkate, S. V. Tiwari and C. H. Gill, *J. Heterocycl. Chem.*, 2018, **55**, 2297–2302; (*b*) V. S. Dofe, A. P. Sarkate, Z. M. Shaikh, C. K. Jadhav, A. S. Nipte and C. H. Gill, *J. Heterocycl. Chem.*, 2018, **55**, 756–762; (*c*) S. Samanta, A. K. Ghosh, S. Ghosh, A. A. Ilina, Y. A. Volkova, I. V. Zavarzin, A. M. Scherbakov, D. I. Salnikova, Y. U. Dzichenka and A. B. Sachenko, *Org. Biomol. Chem.*, 2020, **18**, 5571–5576.
24 A. Shaabani, R. Afshari, S. E. Hooshmand and M. Keramati Nejad, *ACS Sustainable Chem. Eng.*, 2017, **5**, 9506–9516.
25 S. Das Sharma, P. Hazarika and D. Konwar, *Tetrahedron Lett.*, 2008, **49**, 2216–2220.
26 A. Teimouri and A. N. Chermahini, *J. Mol. Catal. A: Chem.*, 2011, **346**, 39–45.
27 E. Kanaani and M. Nasr-Esfahani, *J. Chin. Chem. Soc.*, 2019, **66**, 119–125.
28 Y. Gu, *Green Chem.*, 2012, **14**, 2091–2128.
29 Y. L. Wang, J. Luo and Z. L. Liu, *J. Chin. Chem. Soc.*, 2013, **60**, 1007–1013.
30 (*a*) S. Fujihara, T. Kato and T. Kimura, *J. Sol-Gel Sci. Technol.*, 2003, **26**, 953–956; (*b*) E. Kemnitz and J. Noack, *Dalton Trans.*, 2015, **44**, 19411–19431.
31 V. Sage, J. H. Clark and D. J. Macquarrie, *J. Catal.*, 2004, **227**, 502–511.
32 Y. A. Opata and J. C. Grivel, *J. Anal. Appl. Pyrolysis*, 2018, **132**, 40–46.
33 S. I. Gutnikov, E. V. Karpova, M. A. Zakharov and A. I. Boltalin, *Russ. J. Inorg. Chem.*, 2006, **51**, 541–548.
34 K. Mantri, K. Komura, Y. Kubota and Y. Sugi, *J. Mol. Catal. A: Chem.*, 2005, **236**, 168–175.
35 L. Xu, Y. Zhang, J. Zhang, J. Liu, Y. Shi, Y. Li, G. Dang, Y. Cheng, N. Chen and A. Guo, *Minerals*, 2020, **72**, 1–25.
36 (*a*) C. Khatri, D. Jain and A. Rani, *Fuel*, 2010, **89**, 3853–3859; (*b*) A. Rani, C. Khatri and R. Hada, *Fuel Process. Technol.*, 2013, **116**, 366–373.
37 M. Kidwai, P. Mothsra, V. Bansal and R. Goyal, *Monatsh. Chem.*, 2006, **137**, 1189–1194.
38 H. Naeimi and D. Aghaseyedkarimi, *New J. Chem.*, 2015, **39**, 9415–9421.
39 S. Balalaie, A. Arabanian and M. S. Hashtroudi, *Monatsh. Chem.*, 2000, **131**, 945–948.
40 A. Teimouri and A. N. Chermahini, *J. Mol. Catal. A: Chem.*, 2011, **346**, 39–45.
41 G. V. M. Sharma, Y. Jyothi and P. S. Lakshmi, *Synth. Commun.*, 2006, **36**, 2991–3000.
42 H. D. Hanoon, S. M. Radhi and S. K. Abbas, *AIP Conf. Proc.*, 2019, **2144**, 020005.
43 A. Marzouk, V. M. Abbasov, A. H. Talybov and S. K. Mohamed, *World. J. Org. Chem.*, 2013, **1**, 6–10.
44 H. Zheng, Q. Y. Shi, K. Du, Y. J. Mei and P. F. Zhang, *Catal. Lett.*, 2013, **143**, 118–121.
45 S. A. Siddiqui, U. C. Narkhede, S. S. Palimkar, T. Daniel, R. J. Lahoti and K. V. Srinivasan, *Tetrahedron*, 2005, **61**, 3539–3546.
46 M. Esmaeilpour, J. Javidi and M. Zandi, *New J. Chem.*, 2015, **39**, 3388–3398.
47 J. Safari and Z. Zarnegar, *Ultrason. Sonochem.*, 2013, **20**, 740–746.
48 H. D. Hanoon, E. Kowsari, M. Abdouss, M. H. Ghasemi and H. Zandi, *Res. Chem. Intermed.*, 2017, **43**, 4023–4041.
49 L. Wang and C. Cai, *Monatsh. Chem.*, 2009, **140**, 541–546.
50 B. F. Mirjalili, A. Bamoniri and M. A. Mirhoseini, *Sci. Iran.*, 2013, **20**, 587–591.
51 A. Shaabani, A. Maleki and M. Behnam, *Synth. Commun.*, 2009, **39**, 102–110.
52 H. Weinmann, M. Harre, K. Koenig, E. Merten and U. Tilstam, *Tetrahedron Lett.*, 2002, **43**, 593–595.
53 R. Wang, C. Liu and G. Luo, *Green Chem. Lett. Rev.*, 2010, **3**, 101–104.
54 S. S. Dipake, M. K. Lande, A. S. Rajbhoj and S. T. Gaikwad, *Res. Chem. Intermed.*, 2021, **47**, 2245–2261.